Supporting Online Material for

Perceptual Learning Incepted by Decoded fMRI Neurofeedback Without Stimulus Presentation

Kazuhisa Shibata, Takeo Watanabe,* Yuka Sasaki, Mitsuo Kawato

*To whom correspondence should be addressed. E-mail: takeo@bu.edu

Published 9 December 2011, *Science* **334**, 1413 (2011)
DOI: 10.1126/science.1212003

This PDF file includes:

Materials and Methods

The complete experiment consisted of 4 stages: pre-test (1 day), fMRI decoder construction (1 day), induction (decoded fMRI neurofeedback, 5 days for 4 subjects and 10 days for 6 subjects), and post-test (1 day) stages (Fig. 1A). Different stages were separated by at least 24 hours.

Subjects

Sixteen naïve subjects (20 to 38 years old; 11 males and 5 females) with normal or corrected-to-normal vision participated in the study. All the experiments and data analyses were conducted in Advanced Telecommunications Research Institute International (ATR). The study was approved by the Institutional Review Board of ATR. All subjects gave written informed consents.

Pre- and post-test stages

Only behavioral data were collected in the pre- and post-test stages. Oriented Gabor patches (spatial frequency=1 cycle/deg, contrast=100%, sigma of its Gaussian filter=2.5 deg, random spatial phase) were presented within an annulus subtending 0.75 to 5 deg from the center of a gray screen and were spatially masked by noise, which was generated from a sinusoidal luminance distribution, at a certain signal to noise (S/N) ratio (*21*). For example, in the case of 12% S/N ratio, 88% of pixels of a Gabor patch were replaced by noise.

Subjects' discrimination performance for the Gabor patches was measured (Fig. 1B) before (pre-test stage) and after (post-test stage) the induction stage (see below). In each trial, one of three Gabor orientations (10, 70, 130 deg; Fig. 1C for examples) was presented at one of four S/N ratios (4, 6, 8, 12%). The order of presentations of the orientations and S/N ratios was randomly determined and counterbalanced across trials. Throughout the task, the subjects were asked to fixate their eyes on a white bull's-eye on a gray disc (0.75 deg radius) at the center of the display. Each trial started with a 750-ms fixation period. Then, a Gabor patch was presented for 300 ms, after which the subjects were given 2 sec to report which of 3 possible Gabor orientations was presented by pressing one of 3 buttons on a keyboard. After each trial, a 500-ms inter-trial interval was inserted, consisting of a blank gray background. A brief break period was provided after each run of 50 trials. The subjects conducted 600 trials on each day. The magnitude of performance improvement was defined as the performance in the pre-test subtracted from the performance in the post-test.

FMRI decoder construction stage

The purpose of the fMRI decoder construction stage was to obtain the fMRI signals corresponding to each of three actual orientations, which would then be used to compute the parameters for the decoder used in the later induction stage.

First, we measured subjects' retinotopic maps to delineate visual cortical areas individually using a standard retinotopic method with blood-oxygen-level dependent (BOLD) signal (see elsewhere (*22-24*) for more details; see *MRI parameters* below). In addition, the subjects were presented with a reference stimulus to localize the retinotopic regions in V1/V2 corresponding to the visual field stimulated by the Gabor patches. The

reference stimulus was composed of a colored checkerboard pattern presented within an annulus subtending 1 to 4.75 deg from the center of a gray screen. We used a smaller annular region for the reference stimulus than for the Gabor patches to avoid selecting voxels corresponding to the stimulus edges, which may contain information irrelevant to orientation (*25*).

Next, we measured subjects' BOLD signal patterns (see *MRI parameters* below) for the three Gabor orientations (10, 70, 130 deg) used in the pre- and post-test stages at 50% S/N ratio. Throughout the fMRI run, the subjects were asked to fixate their eyes on a white bull's-eye on a gray disc (0.75 deg radius) presented at the center of the display. The subjects conducted 240 trials in a total of ten fMRI runs. A brief break period was provided after each run upon subjects' requests.

Each fMRI run consisted of 24 task trials (1 trial=12 sec; Fig. 1D), plus a 10-sec fixation period before the trials and 2-sec fixation after the trials (1 run=300 sec). The fMRI data for the initial 10 sec of each run were discarded due to possible unsaturated T1 effects. Each task trial consisted of a stimulus period (6 sec) and a response period (6 sec). At the beginning of each task trial, the color of the fixation point changed from white to green to indicate the start of the stimulus period, during which Gabor patches with one of the three orientations flashed at 1 Hz. Thus, during the stimulus period, the same Gabor orientation was presented 6 times. One of the three Gabor orientations was randomly assigned to each trial. In a half of 24 trials of each fMRI run, the spatial frequency of one of the flashing Gabor patches was slightly increased relative to the other 5 Gabor patches. In the other half, the spatial frequency of the flashing Gabor patches did not change.

The stimulus period was followed by the response period, in which only the fixation point was presented. The color of the fixation point reverted to white. During the response period, the subjects were asked to respond as to whether there was any spatial frequency change in the Gabor patches presented in the prior stimulus period. The subjects were instructed to press the button with their right hand if they detected any spatial frequency change (for example, the second Gabor in Fig. 1D consists of a higher spatial frequency). If subjects did not detect any frequency change, they were instructed not to press the button.

Task difficulty was controlled according to subjects' button responses using an adaptive staircase method (*26*) so that the task difficulty was kept constant throughout trials: the degree of spatial frequency change for the next trial was decreased by 0.02 Hz in the case of a correct detection (hit), and increased by 0.02 Hz in the case of a false alarm or miss. In the case of a correct rejection, the degree of spatial frequency change remained the same. The mean (±s.e.) degree of the spatial frequency change during the task was 0.1174±0.009 Hz, and the mean (±s.e.) task accuracy was 71.3±0.7% across the subjects.

Measured fMRI signals to Gabor orientations and to stimuli for retinotopy were preprocessed using BrainVoyager QX software. All functional images underwent 3D motion correction. No spatial or temporal smoothing was applied. Rigid-body transformations were performed to align the functional images to the structural image for each subject. A gray matter mask was used to extract fMRI data only from gray matter voxels for further analyses.

We conducted a voxel-by-voxel conventional amplitude analysis (*23, 24*) to identify the retinotopic region of V1, V2, and the sub-region that corresponded to the reference stimulus within V1/V2 (the reference region). Once we identified the reference region, time-courses of BOLD signal intensities were extracted from each voxel in the reference region and shifted by 6 sec to account for the hemodynamic delay using the Matlab software. A linear trend was removed from the time-course, and the time-course was z-score normalized for each voxel in each run to minimize baseline differences across the runs. The data samples for computing the decoder were created by averaging the BOLD signal intensities of each voxel for 3 volumes corresponding to the 6-sec stimulus period.

We used a multinomial linear sparse logistic regression, which automatically selected the relevant voxels in the reference region within V1/V2 for decoding (*27, 28*), to construct a decoder for the induction stage. The input voxels were selected from the region of the 1.00 to 4.75 deg eccentricity within V1/V2. Thus, the voxels at the fovea and those that reflected stimulus edges were excluded from the analyses. Because of this exclusion and the usage of the Gabor stimulus with 5 deg radius, T-junctions were doubly avoided as a source of orientation information. We trained the decoder to classify a pattern of BOLD signals into one of three Gabor orientations (10, 70, 130 deg) using 240 data samples obtained from 240 trials in the ten fMRI runs. As a result, the inputs to the decoder were the subjects' moment-to-moment brain activations, while the outputs of the decoder represented the calculated likelihood of each Gabor orientation being presented to the subjects. The mean (±s.e.) number of voxels for decoding was 239±29 in V1/V2.

Induction stage

In the induction stage, which consisted of 5 or 10 daily sessions (but not necessarily consecutive), the subjects were instructed to regulate activation in the posterior part of the brain without any actual visual stimuli presented except for the central fixation point. Debriefing interviews conducted after the experiment confirmed that the subjects were naïve about the function of the posterior part of the brain.

During each neurofeedback day, subjects participated in up to 12 fMRI runs. The mean (±s.e.) number of runs in each day was 10.8±0.3 across days and subjects. Each fMRI run consisted of 15 trials (1 trial=20 sec) preceded by a 30-sec fixation period (1 run=330 sec). The fMRI data for the initial 10 sec were discarded to avoid unsaturated T1 effects. Throughout a run, the subjects were instructed to fixate their eyes on a white bull's-eye at the center of a gray disc (0.75 deg radius) presented at the center of the display. After each run, a brief break period was provided upon a subject's request.

Each trial (Fig. 1E) consisted of an induction period (6 sec), a fixation period (6 sec), a feedback period (2 sec), and an inter-trial interval (6 sec) in this order. During the induction period, the color of the fixation point changed from white to green. No visual stimulus except the fixation point was presented during the induction period. The subjects were instructed to regulate the posterior part of their brains, with the goal of making the size of a solid green disc presented in the later feedback period as large as possible. The experimenters provided no further instructions or strategies. During the fixation period, the subjects were asked simply to fixate on the central point. This period was inserted between the induction period and the feedback period due to the known hemodynamic delay, which we assumed lasted 6 sec, during which V1/V2 activation patterns were

calculated in time for a green disc to be shown in the subsequent feedback period. During the feedback period, the green disc was presented for 2 sec. The size of the disc presented in the feedback period represented how much a momentary BOLD signal pattern in V1/V2 obtained in the prior induction period corresponded to the pattern induced by the presentation of the real and specific targeted Gabor orientation, collected through the above-mentioned fMRI decoder construction stage. The green disc was always enclosed by a larger green concentric circle (5 deg radius), which indicated the disc's maximum possible size. The feedback period was followed by an inter-trial interval that lasted 6 sec, during which the subjects were asked to fixate on a central white point. This period was followed by the start of the next trial.

The target Gabor orientation was randomly selected from one of the three orientations (10, 70, 130 deg) and assigned to each subject without informing the subjects about the assigned target orientation. The remaining two orientations were rotated from -60 deg and +60 deg from the target orientation. The size of the disc presented during the feedback period was computed during the fixation period in the following manner. First, measured functional images during the induction period underwent 3D motion correction using Turbo BrainVoyager. Second, time-courses of BOLD signal intensities were extracted from each of the voxels identified in the fMRI decoder construction stage, and were shifted by 6 sec to account for the hemodynamic delay. Third, a linear trend was removed from the time-course, and the BOLD signal time-course was z-score normalized for each voxel using BOLD signal intensities measured for 20 sec starting from 10 sec after the onset of each fMRI run. Fourth, the data sample to calculate the size of the disc was created by averaging the BOLD signal intensities of each voxel for 6 sec in the induction period. Finally, the likelihood of each orientation was calculated from the data sample using the decoder computed in the fMRI decoder construction stage. The size of the disc was proportional to the likelihood (ranging from 0 to 100%) of the target orientation assigned to each subject. The target orientation was constant throughout the induction stage.

In addition to a fixed amount of the compensation for participation in the experiment, a bonus of up to $30 was paid to the subjects based on the mean size of the disc in each day.

After post-test stage

When the subjects were asked what they tried to do to increase the size of the feedback disc, the most common reply was: "I tried various things since I had no idea of the correct way". The strategies each subject reported to use were as follows:

Subject 1 " I tried to remember various scenes from one famous animated movie."
Subject 2 "I tried to remember various things that had happened yesterday, or to image I am moving my fingers."
Subject 3 "I tried to keep switching my attention between the two eyes or to imagine a big green disc."
Subject 4 "I tried to focus my attention on the fixation point at the center of the display."
Subject 5 "I tried to obtain and keep an image of a big green disc."
Subject 6 "I tried to keep my attention on the back part of my brain."
Subject 7 "I tried to focus my attention on the color of the fixation point at the center of the display."

Subject 8 “I tried to imagine a big green disc.”
Subject 9 “I tried to imagine a big green disc.”
Subject 10 “I tried to remember old memories or to perform numerical calculation.”

Apparatus and stimuli

Visual stimuli were presented on a LCD display (1024 × 768 resolution, 60 Hz refresh rate) during the pre- and post-test stages and via a LCD projector (1024 × 768 resolution, 60 Hz refresh rate) during fMRI measurements in a dim room. All visual stimuli were made using Matlab and Psychtoolbox 3 (*29*) on Mac OS X.

MRI parameters

The subjects were scanned in a 3T MR scanner with a head coil in the ATR Brain Activation Imaging Center. Retinotopy, fMRI signals for the fMRI decoder construction and induction stages were acquired using a gradient EPI sequence. In all fMRI experiments, 33 contiguous slices (TR=2 sec, voxel size=3 × 3 × 3.5 mm^3, 0 mm slice gap) oriented parallel to the AC-PC plane were acquired, covering the entire brain. For an inflated format of the cortex used for retinotopic mapping and an automated parcellation method (*30*), T1-weighted MR images (MP-RAGE; 256 slices, voxel size=1 × 1 × 1 mm^3, 0 mm slice gap) were also acquired during the decoder construction stage.

Control experiment

The purpose of the control experiment was to test whether participating in the pre- and post-test stages alone was sufficient to improve subjects’ discrimination performance, without an induction stage. Thus, the control experiment consisted only of the pre- and post-test stages. The procedure was otherwise identical to that of the main experiment. Since the average interval between the pre- and post-test stages in the main experiment with 10-day induction stage was 28 days, the interval between the pre- and post-test stages in the control experiment was also set to this length.

Offline tests

We conducted two offline tests for the following 5 additional brain areas: V3, V4, the intraparietal sulcus (IPS), the lateral prefrontal cortex (LPFC), and the combined region from V3 to LPFC. Localizations of V3 and V4 were determined based on individual retinotopic maps. Localizations of IPS and LPFC were determined based on anatomical landmarks derived from an automated brain parcellation method (*30*). LPFC was anatomically defined as the middle frontal gyrus plus the inferior frontal sulcus.

In the first offline test, a sparse linear regression (*31*) was applied to predict a neurofeedback signal (i.e., likelihood of the target orientation in V1/V2 during the induction stage) from an activation pattern in each of the 5 areas mentioned above for each trial of the induction stage, and an activation pattern from the V1/V2 itself as a control. Note that the output of the sparse logistic regression decoder (i.e., likelihood of the target orientation in V1/V2; ranging from 0 to 100%) had been computed using a non-linear function (logistic function) (*28*). Thus, before applying the sparse linear regression for each area, the likelihoods in V1/V2 were linearized using an arc hyperbolic tangent function. A predicted value was obtained as the linearly weighted sum of the voxel activities in each area. Prediction accuracy was defined as a coefficient of

determination and evaluated by a leave-one-day-out cross validation procedure. That is, the pair of the V1/V2 likelihoods and the activation patterns for each area measured on one day during the induction stage were treated as the test data while those measured on the remaining days were used for training the sparse linear regression decoder to predict trial-by-trial likelihoods in V1/V2. Five or ten cross-validation sets were generated. A coefficient of determination here indicates the proportion of variability in the likelihoods on a trial-by-trial basis in V1/V2 that is explained by voxel activities in each area. The coefficient of determination for each area was first averaged over the cross-validation sets and then across the subjects and is shown in Fig. S9A. The coefficient for V1/V2 itself was 71% and high, but those for the other 5 areas were les than 5%. The numbers of voxels selected by the sparse algorithm to obtain the predicted values were 371±32 (V1/V2), 203±13 (V3), 259±11 (V4), 629±24 (IPS), and 812±67 (LPFC), respectively.

In the second offline test, we constructed five multinomial sparse logistic regression decoders (*28*) for V3, V4, IPS, LPFC, and the combined region from V3 to LPFC. The entire procedure was the same as described for the fMRI decoder construction stage in the main text. Using the same procedure as for V1/V2, decoding accuracy was evaluated using a leave-one-run-out cross validation procedure for each of the 5 areas. Ten cross-validation sets were generated for each area, and accuracies for the sets were first averaged over the cross-validation sets and then across the subjects. Fig. S9B shows the results of these 5 areas as well as that from V1/V2 as a control. The numbers of voxels selected by the sparse algorithm for decoding were 239±29 (V1/V2), 178±25 (V3), 194±15 (V4), 235±30 (IPS), and 223±13 (LPFC), respectively.

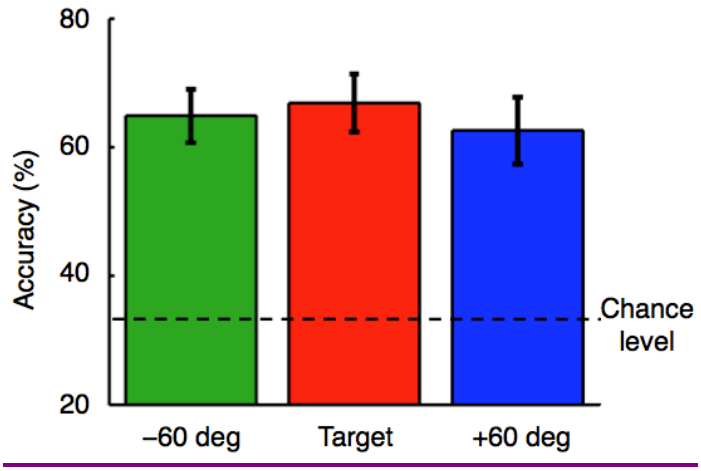

Fig. S1. Performance of a decoder for V1/V2. A leave-one-run-out cross validation procedure (*28*) confirmed that the decoder successfully predicts the Gabor orientations presented to the subjects based on the fMRI datasets measured in the fMRI decoder construction stage. The mean accuracy (±s.e.) for each orientation was significantly higher than the 33% chance level ($t(9)>6.98$, $P<10^{-4}$).

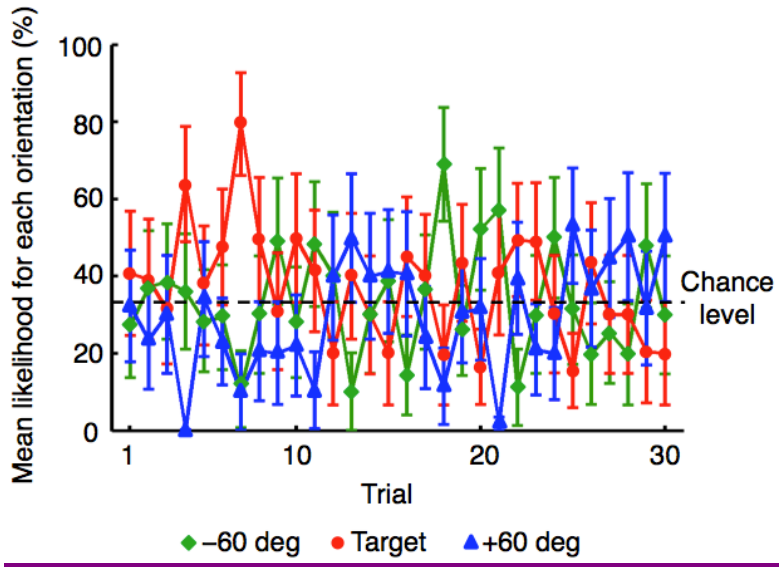

Fig. S2. The mean (±s.e.) likelihood of each of three orientations in the first 30 trials of the first day in the induction stage.

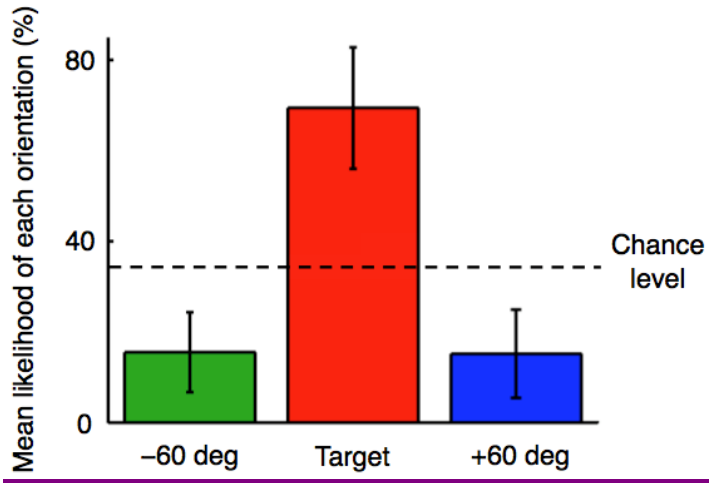

Fig. S3. Results of decoding analysis to the overall mean activation pattern. We also applied the same decoder to the overall mean activation pattern, rather than trial-by-trial activation patterns, in V1/V2 during the induction stage for each subject. Consistent with the results of trial-by-trial decoding, the mean target-orientation likelihood was significantly higher than chance level ($t(9)=2.69$, $P=0.02$).

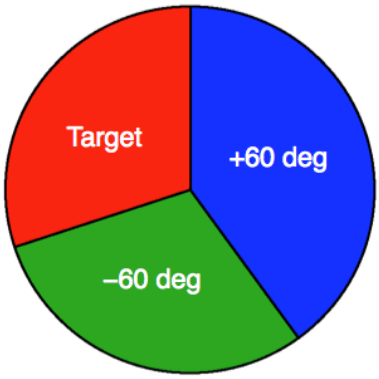

Fig. S4. The percentages of orientations chosen as the target orientation by subjects. The percentages were statistically undistinguishable from what would be expected from chance (Chi-square test, χ^2=0.20, P=0.90).

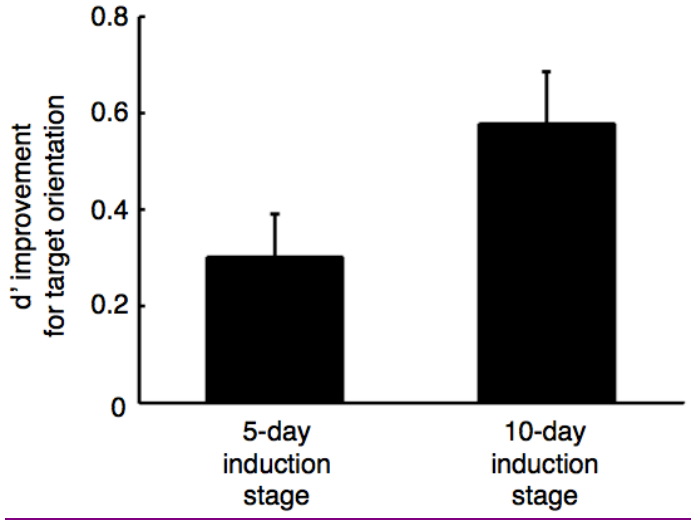

Fig. S5. The mean (±s.e.) d' improvements for the target orientation at 6% S/N ratio. Significant improvements were found for both subjects who participated in 5-day induction stage (left, $t(3)=3.38$, $P=0.04$) and the subjects in 10-day induction stage (right, $t(5)=5.36$, $P<10^{-2}$). No significant difference was found between the two groups (left, $t(8)=1.81$, $P=0.11$).

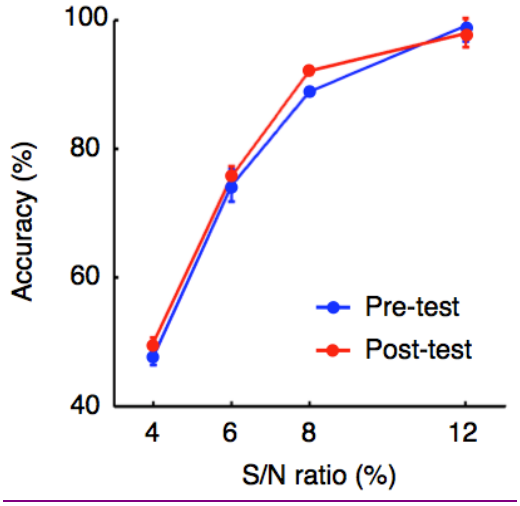

Fig. S6. Results of the pre- and post-tests in the control experiment (n=6) with no induction stage. This plot shows the mean (±s.e.) discrimination accuracies across 10 deg, 70 deg, and 130 deg in the pre- and post-tests as a function of the S/N ratio. Two-way (test stage x S/N ratio) ANOVA with repeated measures indicate no significant effect of test stage ($F(1, 5)=3.25$, $P=0.13$) or interaction of test stage and S/N ratio ($F(3, 15)=1.71$, $P=0.21$).

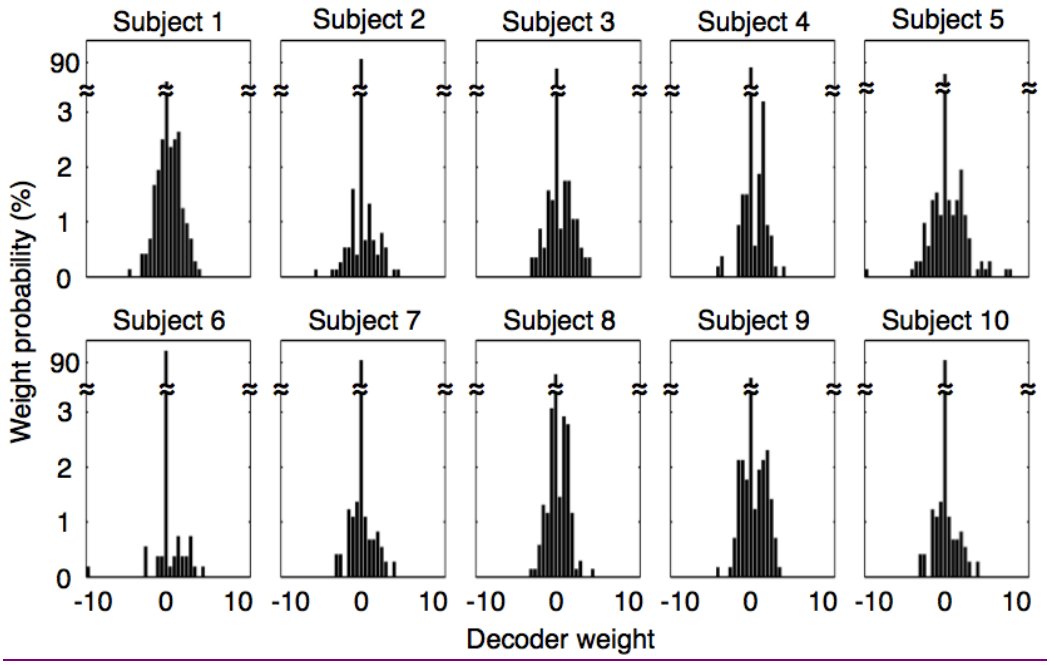

Fig. S7. Histograms of decoder weights for the target orientation in V1/V2 voxels for each subject. Multinomial sparse logistic regression automatically selected relevant voxels, which were informative (decoder weights not being zero) to decode the Gabor orientations, based on fMRI datasets in the fMRI decoder construction stage. The histograms show that about 13% of voxels were assigned to non-zero decoder weights, which were distributed to both positive and negative values. Thus, the high likelihoods computed for the target orientations cannot be obtained simply by increasing global activation in V1/V2.

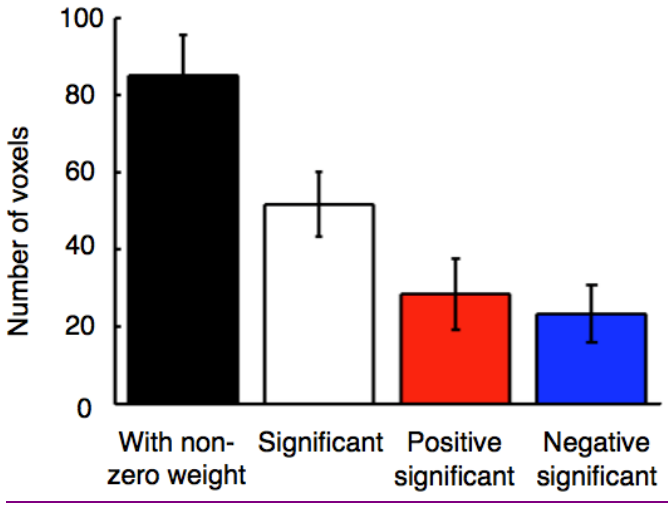

Fig. S8. The mean (±s.e.) number of voxels that showed significant activation during the induction stage. On average, 85 voxels were assigned to non-zero weight (black bar), and 52 of those voxels had significant activation (white bar; t-test, $P<0.05$, corrected by the number of voxels). Approximately, half of the significant voxels were activated positively (red bar) while the other half were activated negatively (blue bar).

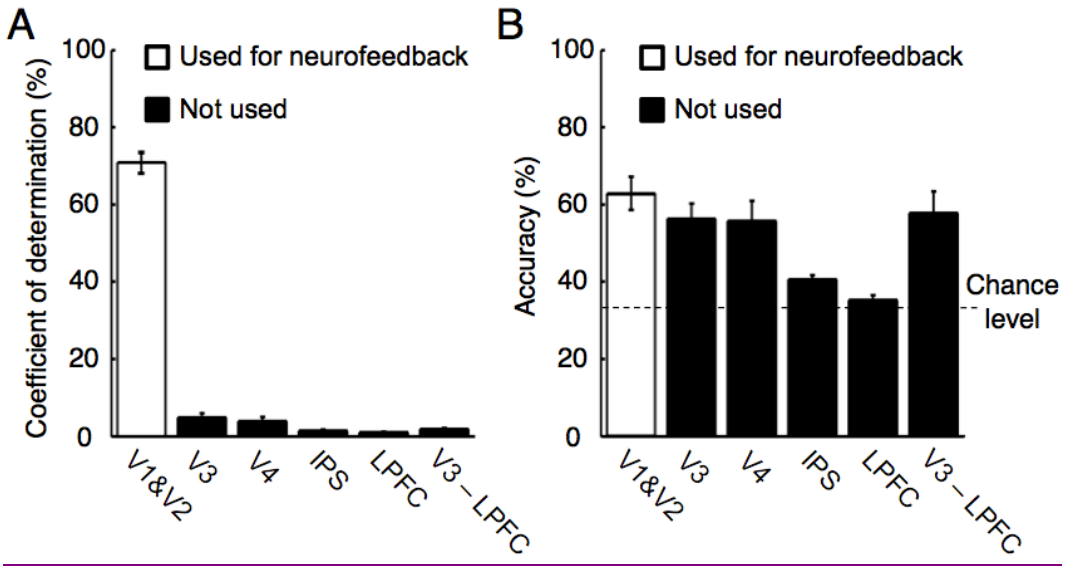

Fig. S9. Results of two offline tests. (A) The mean (±s.e.) coefficient of determination (goodness of fits between the likelihood in V1/V2 and its predicted value for each area, multiplied by 100) for the sparse-linear-regression prediction by each of activation patterns in V3, V4, intraparietal sulcus (IPS), lateral prefrontal cortex (LPFC), and V3-LPFC combined region during the induction stage, and from the V1/V2 itself as a control. The mean coefficients of determination were less than 5% in the 5 areas other than V1/V2. (B) Performance of a multinomial sparse regression decoder for each of the 6 areas including V1/V2 in the fMRI decoder construction stage. Two-way (orientation x area) ANOVA with repeated measures showed significant effect of area ($F(5, 45)=15.01$, $P<10^{-4}$) but no significant effect of orientation ($F(2, 18) = 1.70$, $P = 0.21$) and interaction between area and orientation ($F(10, 90)=1.19$, $P=0.31$) on decoding accuracies. Thus, the accuracies for the 3 orientations were averaged. Results indicated that the decoder successfully predicted the Gabor orientations presented to the subjects based on the fMRI datasets measured in the fMRI decoder construction stage for the areas V1/V2 ($t(9)=6.98$, $P=10^{-4}$), V3 ($t(9)=6.25$, $P < 10^{-3}$), V4 ($t(9)=4.42$, $P<10^{-2}$), IPS ($t(9)=7.50$, $P<10^{-4}$), LPFC ($t(9)=2.69$, $P=0.02$), and V3-LPFC combined region ($t(9)=4.81$, $P<10^{-3}$).

References and Notes

1. A. Schoups, R. Vogels, N. Qian, G. Orban, Practising orientation identification improves orientation coding in V1 neurons. *Nature* **412**, 549 (2001). doi:10.1038/35087601 Medline

2. Y. Yotsumoto, T. Watanabe, Y. Sasaki, Different dynamics of performance and brain activation in the time course of perceptual learning. *Neuron* **57**, 827 (2008). doi:10.1016/j.neuron.2008.02.034 Medline

3. T. Hua *et al*., Perceptual learning improves contrast sensitivity of V1 neurons in cats. *Curr. Biol.* **20**, 887 (2010). doi:10.1016/j.cub.2010.03.066 Medline

4. N. Censor, Y. Bonneh, A. Arieli, D. Sagi, Early-vision brain responses which predict human visual segmentation and learning. *J. Vision* **9**, 1 (2009). doi:10.1167/9.4.12 Medline

5. A. Karni, D. Sagi, The time course of learning a visual skill. *Nature* **365**, 250 (1993). doi:10.1038/365250a0 Medline

6. C. T. Law, J. I. Gold, Neural correlates of perceptual learning in a sensory-motor, but not a sensory, cortical area. *Nat. Neurosci.* **11**, 505 (2008). doi:10.1038/nn2070 Medline

7. T. Yang, J. H. Maunsell, The effect of perceptual learning on neuronal responses in monkey visual area V4. *J. Neurosci.* **24**, 1617 (2004). doi:10.1523/JNEUROSCI.4442-03.2004 Medline

8. C. M. Lewis, A. Baldassarre, G. Committeri, G. L. Romani, M. Corbetta, Learning sculpts the spontaneous activity of the resting human brain. *Proc. Natl. Acad. Sci. U.S.A.* **106**, 17558 (2009). doi:10.1073/pnas.0902455106 Medline

9. O. Yamashita, M. A. Sato, T. Yoshioka, F. Tong, Y. Kamitani, Sparse estimation automatically selects voxels relevant for the decoding of fMRI activity patterns. *Neuroimage* **42**, 1414 (2008). doi:10.1016/j.neuroimage.2008.05.050 Medline

10. S. Bray, S. Shimojo, J. P. O'Doherty, Direct instrumental conditioning of neural activity using functional magnetic resonance imaging-derived reward feedback. *J. Neurosci.* **27**, 7498 (2007). doi:10.1523/JNEUROSCI.2118-07.2007 Medline

11. A. Caria *et al*., Regulation of anterior insular cortex activity using real-time fMRI. *Neuroimage* **35**, 1238 (2007). doi:10.1016/j.neuroimage.2007.01.018 Medline

12. R. C. deCharms *et al*., Learned regulation of spatially localized brain activation using real-time fMRI. *Neuroimage* **21**, 436 (2004). doi:10.1016/j.neuroimage.2003.08.041 Medline

13. N. Weiskopf *et al*., Physiological self-regulation of regional brain activity using real-time functional magnetic resonance imaging (fMRI): Methodology and exemplary data. *Neuroimage* **19**, 577 (2003). doi:10.1016/S1053-8119(03)00145-9 Medline

14. A. Toda, H. Imamizu, M. Kawato, M. A. Sato, Reconstruction of two-dimensional movement trajectories from selected magnetoencephalography cortical currents by combined sparse Bayesian methods. *Neuroimage* **54**, 892 (2011). doi:10.1016/j.neuroimage.2010.09.057 Medline

15. K. R. Huxlin *et al*., Perceptual relearning of complex visual motion after V1 damage in humans. *J. Neurosci.* **29**, 3981 (2009). doi:10.1523/JNEUROSCI.4882-08.2009 Medline

16. E. Corthout, B. Uttl, V. Walsh, M. Hallet, A. Cowey, Plasticity revealed by transcranial magnetic stimulation of early visual cortex. *Neuroreport* **11**, 1565 (2000). doi:10.1097/00001756-200005150-00039 Medline

17. F. Giovannelli *et al*., Involvement of the parietal cortex in perceptual learning (Eureka effect): An interference approach using rTMS. *Neuropsychologia* **48**, 1807 (2010). doi:10.1016/j.neuropsychologia.2010.02.031 Medline

18. H. R. Dinse, P. Ragert, B. Pleger, P. Schwenkreis, M. Tegenthoff, Pharmacological modulation of perceptual learning and associated cortical reorganization. *Science* **301**, 91 (2003). doi:10.1126/science.1085423 Medline

19. Y. Miyashita, Cognitive memory: Cellular and network machineries and their top-down control. *Science* **306**, 435 (2004). doi:10.1126/science.1101864 Medline

20. M. Kawato, From 'understanding the brain by creating the brain' towards manipulative neuroscience. *Philos. Trans. R. Soc. London Ser. B* **363**, 2201 (2008). doi:10.1098/rstb.2008.2272 Medline

21. A. R. Seitz, D. Kim, T. Watanabe, Rewards evoke learning of unconsciously processed visual stimuli in adult humans. *Neuron* **61**, 700 (2009). doi:10.1016/j.neuron.2009.01.016 Medline

22. S. A. Engel, G. H. Glover, B. A. Wandell, Retinotopic organization in human visual cortex and the spatial precision of functional MRI. *Cereb. Cortex* **7**, 181 (1997). doi:10.1093/cercor/7.2.181 Medline

23. D. Fize *et al*., The retinotopic organization of primate dorsal V4 and surrounding areas: A functional magnetic resonance imaging study in awake monkeys. *J. Neurosci.* **23**, 7395 (2003). Medline

24. Y. Yotsumoto *et al*., Location-specific cortical activation changes during sleep after training for perceptual learning. *Curr. Biol.* **19**, 1278 (2009). doi:10.1016/j.cub.2009.06.011 Medline

25. Y. Kamitani, F. Tong, Decoding the visual and subjective contents of the human brain. *Nat. Neurosci.* **8**, 679 (2005). doi:10.1038/nn1444 Medline

26. S. Nishida, Y. Sasaki, I. Murakami, T. Watanabe, R. B. Tootell, Neuroimaging of direction-selective mechanisms for second-order motion. *J. Neurophysiol.* **90**, 3242 (2003). doi:10.1152/jn.00693.2003 Medline

27. Y. Miyawaki *et al*., Visual image reconstruction from human brain activity using a combination of multiscale local image decoders. *Neuron* **60**, 915 (2008). doi:10.1016/j.neuron.2008.11.004 Medline

28. O. Yamashita, M. A. Sato, T. Yoshioka, F. Tong, Y. Kamitani, Sparse estimation automatically selects voxels relevant for the decoding of fMRI activity patterns. *Neuroimage* **42**, 1414 (2008). doi:10.1016/j.neuroimage.2008.05.050 Medline

29. D. H. Brainard, The psychophysics toolbox. *Spat. Vision* **10**, 433 (1997). doi:10.1163/156856897X00357 Medline

30. B. Fischl *et al*., Automatically parcellating the human cerebral cortex. *Cereb. Cortex* **14**, 11 (2004). doi:10.1093/cercor/bhg087 Medline

31. A. Toda, H. Imamizu, M. Kawato, M. A. Sato, Reconstruction of two-dimensional movement trajectories from selected magnetoencephalography cortical currents by combined sparse Bayesian methods. *Neuroimage* **54**, 892 (2011). doi:10.1016/j.neuroimage.2010.09.057 Medline